Supporting information

Electrospinning Synthesis of Transition Metal Alloy Nanoparticles Encapsulated in Nitrogen-doped Carbon Layers as an Advanced Bifunctional Oxygen Electrode

Feng Cao[1], Xi Yang[1], Chen Shen[1], Xin Li[1], Jianmin Wang[1], Gaowu Qin[1], Song Li[*1], Xueyong Pang[*1] and Guoqing Li[*2]

[1]Key Lab for Anisotropy and Texture of Materials (MoE), School of Materials Science and Engineering, Northeastern University, Shenyang 110819, China; [2]Department of Materials Science and Engineering, North Carolina State University, Raleigh, NC 27695

* To whom correspondence should be addressed.
Emails: lis@atm.neu.edu.cn; pangxy@atm.neu.edu.cn; gli4@ncsu.edu

Supporting Information 1: Experimental part

1. Synthesis of metal alloy nanoparticles encapsulated by N-doped Carbon fibers.

The reagents used in the experiment were purchased from Sinopharm Chemical Reagent Co., Ltd. Typically, $Fe(NO_3)_3 \cdot 9H_2O$(0.673g), $Ni(NO_3)_2 \cdot 6H_2O$ (0.485g), and $Co(NO_3)_2 \cdot 6H_2O$ (0.485g) were dissolved in dimethylformamide (DMF, 10 mL) that contained polyvinylpyrrolidone (PVP K-30, 5g).The mixture was stirred continuously overnight at room temperature to obtain the homogeneous metal/polymer precursor solution. Next, the as-obtained metal/polymer precursor was transferred into an injection syringe. Thenin the electrospinning process, DC voltage of 17 kV was applied between the injector and the receiver plate at a receiving distance of 15 cm and a solution feed rate of 0.5 $mL \cdot h^{-1}$. The obtained nanofibers were pretreated in air at 250 °C for 2 hours, and then carbonized at 800 °C for 2 hours under Ar/H_2(5%) atmosphere. After calcination, the target product NiCoFe@N-CNFs nanofibers were successfully synthesized.By varying the amount of metal precursors used in the reaction and keeping the same amount of metal/polymer precursors with various metal cation ratios were obtained and then treated at 800 °C for 2h in Ar/H_2 (5%) atmosphere to investigate the influence of the metal ratios on their activity. In addition, the precursor, which was used for the preparation of the NiCoFe@N-CNFs nanofibers material, was treated thermally at 700 °C, 750 °C, or 850 °C for 2h in an Ar/H_2(5%) atmosphere to investigate the influence of the synthesis temperature on the activity.

2. Characterizations

X-Ray diffraction (XRD) was characterized by a Rigaku Smart Lab X-ray diffractometer with CuKa irradiation. The samples were characterized by transmission electron microscopy (TEM) with JEM-2100F and by scanning electron microscopy (SEM) with a JSM-6500F equipped with an energy-dispersive X-ray (EDX) spectrometer at a voltage of 15 kV. The surface

chemical state was analyzed by X-ray photoelectron spectroscopy (XPS, Thermal Scientific K Alpha).

Electrochemical Characterization: All electrochemical measurements were carried out using a three-electrode system with an electrochemical workstation (Zahner iM6e). Hg/HgO electrode was used as the reference electrode and a graphite rod was used as the counter electrode. 5 mg of samples and 5 μL 5% Nafion solution were put in 0.8 mL mixture of water/ethanol with a volume ratio of 3:1 and dispersed by ultrasonication for 30 min to form a homogeneous ink. For OER catalytic performance testing, 5 μL of this ink was carefully dropped onto a glassy carbon electrode (GCE) with a diameter of 3 mm and dried in air. Line sweep voltammograms (LSV) polarization curves were recorded with a scan rate of 5 mV s-1 over a potential range of 1.0 to 2.0 V vs. RHE in 1 M KOH. For ORR catalytic performance testing, 15 μL of this ink was carefully dropped onto a rotating ring disc electrode (RRDE) (carbon disk with surface area of 0.2475 cm^2 surrounded by a Pt ring with a surface area of 0.1866 cm^2) and dried in air. ORR activity and selectivity were investigated by polarization curves and rotating ring disk measurements in oxygen-saturated electrolytes at a scan rate of 10 mV s^{-1}. The polarization curve in the nitrogen-saturated electrolyte was also recorded. Cyclic voltammograms (CV) at various scan rates (10, 20, 30, 40, 50 mV/s) were collected in the -0.1−0.05 V vs RHE range. Double-layer capacitance (Cdl) can be estimated by CV measures. The electrochemical impedance spectroscopy (EIS) measurements were carried out at a potential of 1.55 V vs. RHE with frequencies of 0.1 Hz to 100 000 Hz and an amplitude of 5 mV. An equivalent Randles circuit model was fit to the data to determine the system resistance and capacitance.

Zn–air battery assembly and test: the rechargeable Zn–air battery performance was tested using a homemade Zn–air battery. A Zn–air battery was fabricated using carbon sheets coated with a NiCoFe@N-CNFs catalyst (1 mg cm^{-2}) as the air electrode, Zn foil as the anode, and a 6 M KOH and 0.2 M $Zn(Ac)_2$ aqueous solution as the electrolyte. The potential–current polarization curves for the batteries were recorded on a CHI 760e workstation. The discharge/charge performance and stability for the batteries were analyzed by a Lanhe-CT 2001A testing system at room temperature.

3. Theoretical calculation

Density functional theory (DFT) calculations were carried out using the Generalized Gradient Approximation (GGA) exchange-correlation functional in the Perdew-Burke-Ernzerhof (PBE) equation as implemented in the Vienna ab initio simulation package (VASP).[25] The cut-off energies for plane waves was set at 400 eV, and the energy convergence tolerance was set as 10−5 eV, and the geometry optimization process was performed using a conjugate-gradient algorithm until the final force on each atom was less than 0.01 eV/Å, spin polarization was included in all calculations as well as all magnetic ions were initialized ferromagnetically. We optimized the unit cell of fcc binary and ternary Ni-based alloy, obtained from the unit cell of fcc nickel, substituted of two nickel atoms by two metal atoms. Note that the stoichiometric ratio of Ni, Fe and Co was kept as 1:1:1. The Ni (111) facet was selected as the terminating surface of the slab since the Ni (111) surface is the most active facet for fcc Ni. We constructed a four-atomic-layer model for Ni, NiFe, NiCo, NiCoFe, $NiCo_3Fe$ and calculated

the d-band center. The atoms in the top two layers were fully relaxed while those in the last two layers were fixed to simulate the bulk. To avoid interactions between periodic images, a vacuum layer of 15 Å is added to the adjacent slabs in both models.

Supporting information 2: The detailed calculation of ECSA.

In detail, The ECSA was evaluated by measuring the double layer capacitance method via CVs at different scan rate from 10 to 50 mV s−1 in the range of no Faradaic processes occurred. The electrochemical double-layer capacitance was given according to the following Equation

Cdl = —

where Cdl is the double-layer capacitance, Ic is the charging current, and v is the scan rate.

The number of electrons transferred was calculated using the K–L equations.

$$\frac{1}{j} = \frac{1}{j_k} + \frac{1}{Bw^{0.5}}$$

$$B = 0.2nF(D_{O_2})^{2/3}v^{-1/6}C_{O_2}$$

where j is the measured current density; j_K are the kinetic current density and; ω is the angular velocity of the disk; n represents the overall number of electrons transferred in oxygen reduction; F is the Faraday constant (F = 96485 C mol^{-1}); C_{O2} is the bulk concentration of O_2 (1.2×10−6 mol cm–3); D_{O2} is the diffusion coefficient of O_2 in 0.1 M KOH electrolyte (1.9 × 10−5 cm2 s-1); ν is the kinematics viscosity for electrolyte, and k is the electron-transferred rate constant.

For RRDE tests, a computer-controlled CHI 760E electrochemical workstation was employed and the disk electrode was scanned catholically at a rate of 10 mV s^{-1}. The hydrogen peroxide yield (H2O2 %) and the electron transfer number (n) were determined by the following equations:

—

—

—

—

—

where Id is the disk current, I_r is the ring current, and N = 0.37 is the current collection efficiency of the Pt ring.”

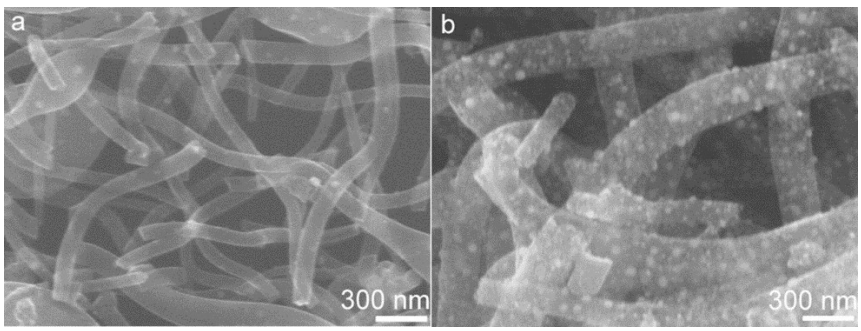

Fig.S1 SEM images of the samples prepared for different precursor concentration (a) lower than 4 mmol. (b)higher than 4mmol.

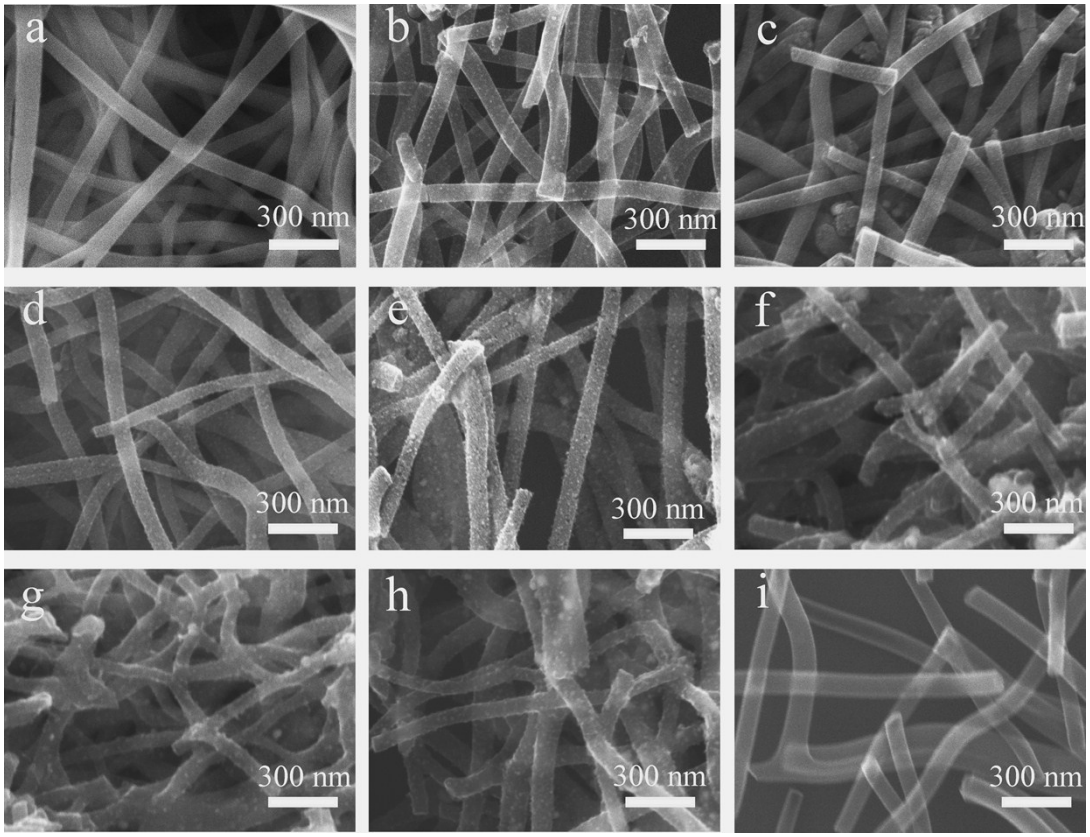

Figure S2 SEM image of Precursor fiber (a), Ni@N-CNFs (b), NiCo@N-CNFs (c), NiFe@N-CNFs (d), CoFe@N-CNFs (e), Ni_3CoFe@N-CNFs (f), $NiCo_3Fe$@N-CNFs (g), $NiCoFe_3$@N-CNFs (h) and N-CNFs (i).

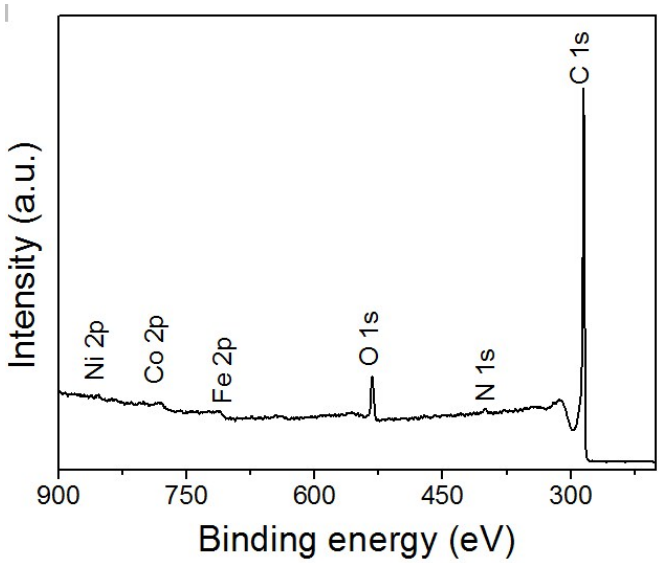

Figure S3. Survey spectrum of NiCoFe@N-CNFs.

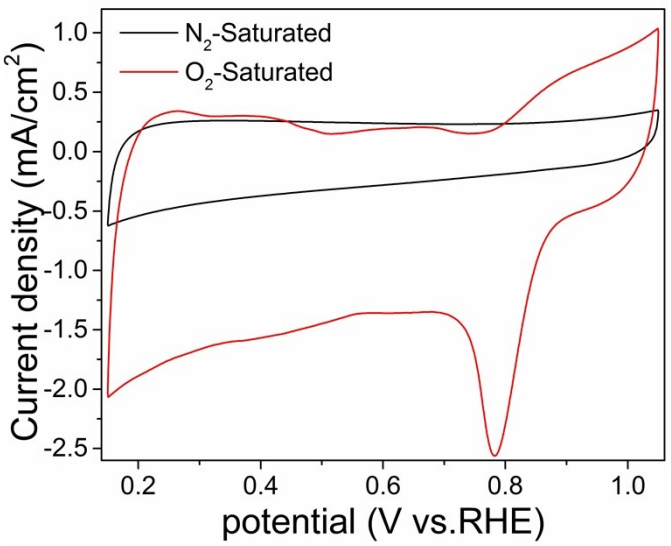

Figure S4. CV curves of NiCoFe@N-CNFs in N_2-Saturated and O_2-Saturated 0.1M KOH solution.

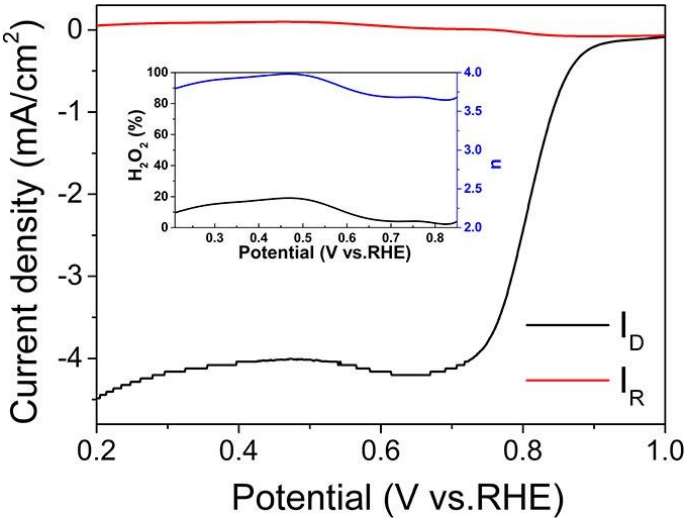

Figure S5. Disk current and ring current curves. Inset: electron transfer number and H_2O_2 yield curves.

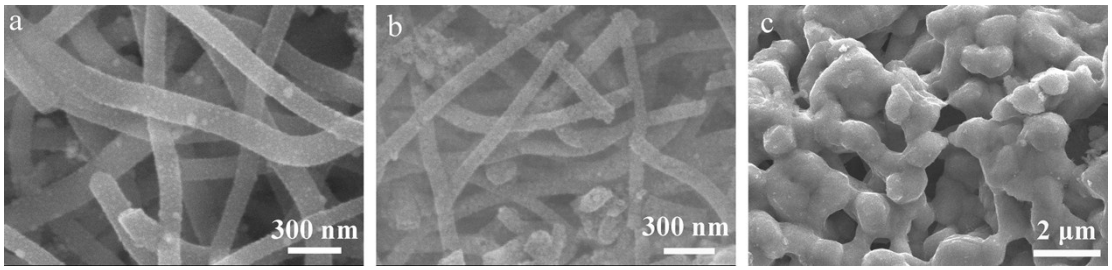

Figure S6. SEM image of NiCoFe-700 (a), NiCoFe-750 (b) and NiCoFe-850 (c).

Table S1. Elemental content of NiCoFe@N-CNFs.

	Atomic %		
Element	EDX	TEM-mapping	XPS
C K	94.98	97.48	98.35
Fe K	1.63	0.86	0.58
Co K	1.71	0.84	0.53
Ni K	1.68	0.82	0.54
Totals	100		

Table S2 Comparison of ORR and OER activity of transition metals-based catalysis in alkaline electrolyte.

Sample	$E_{j=10}$	$E_{halfwave}$	$\Delta E=E_{j=10}-E_{halfwave}$	Renerence
Co@N-CNT	1.62 V	0.84 V	0.78 V	1
Co@N-C	1.601 V	0.742 V	0.859 V	2
NiCo/RFC	1.65 V	0.79 V	0.86 V	3
FeNi@N-C	1.54 V	0.73 V	0.81 V	4
NiCoFe@C	1.58 V	0.85 V	0.73 V	5
$Ni_{46}Co_{40}Fe_{14}$@C	1.66 V	0.73 V	0.93 V	6
NiCoFe@N-CNFs	1.50 V	0.81 V	0.69 V	This work

Table S3. The relationship between precursors' amounts with the proportion of elements in different components of M@N-CNFs wt.%

M@N-CNFs / precures	Ni	CoNi	CoFe	NiFe	NiCoFe	NiCoFeCu	Non-metal
$Fe(NO_3)_3·9H_2O$/g	-	-	1.010	1.010	0.673	0.505	-
$Ni(NO_3)_2·6H_2O$/g	1.453	0.727	-	0.727	0.485	0.363	-
$Co(NO_3)_2·6H_2O$/g	-	0.728	0.728	-	0.485	0.364	-
$Cu(NO_3)_2·3H_2O$/g	-	-	-	-	-	0.302	-
PVP/g	5	5	5	5	5	5	5
DMF/mL	10	10	10	10	10	10	10
$Zn(NO_3)_2·3H_2O$/g	-	-	-	-	-	-	1.487

Table S4: Proportion of elements in different components of M@N-CNFs wt.%

Content / M@N-CNFs	Ni	Co	Fe	Cu
Ni	100	-	-	-
NiCo	51.6	48.4	-	-
NiFe	49.4	-	50.6	-
CoFe	-	51.1	48.9	-
NiCoFe	32.5	34	33.5	-
NiCoFeCu	26.3	24.6	25.2	23.9

Ni_3CoFe	62.1	19.9	21.2	-
$NiCo_3Fe$	19.9	58.0	22.1	-
$NiCoFe_3$	21.2	19.6	59.2	-

Table S5. The comparison between FeNiCo@N-CNFs reported in this work and commercial Pt/C for ORR.

Catalyst	**Onset Potential/V**	**Half Wave/V**	**Saturating Current density /mA/cm^2**
FeNiCo@N-CNFs	0.9V	0.81	4.4
Pt/C	1.0V	0.825	4.6

[1] Liu Y, Jiang H, Zhu Y, et al. Transitional Metal (Fe, Co, Ni) Encapsulated in Nitrogen-Doped Carbon Nanotubes as Bi-functional Catalysts for Oxygen Electrode Reactions[J]. J. Mater. Chem. A, 2016, 4:1694-1701.

[2] Su Y, Zhu Y, Jiang H, et al. Cobalt nanoparticles embedded in N-doped carbon as an efficient bifunctional electrocatalyst for oxygen reduction and evolution reactions[J]. Nanoscale, 2014, 6(24):15080-15089.

[3] Fu G, Chen Y, Cui Z, et al. A Novel Hydrogel-derived Bifunctional Oxygen Electrocatalyst for Rechargeable Air Cathodes[J]. Nano Letters, 2016, 16:6516-6522.

[4] Zhong H X, Wang J, Zhang Q, et al. In Situ Coupling FeM (M = Ni, Co) with Nitrogen-Doped Porous Carbon toward Highly Efficient Trifunctional Electrocatalyst for Overall Water Splitting and Rechargeable Zn-Air Battery[J]. Advanced Sustainable Systems, 2017, 1(6):1700020-1700025.

[5] Versatile electrocatalytic processes realized by Ni, Co and Fe alloyed core coordinated carbon shells[J]. Journal of Materials Chemistry A, 2019, 7:12154-12165.

[6] Nam G , Son Y , Park S O , et al. A Ternary Ni46 Co40 Fe14 Nanoalloy-Based Oxygen Electrocatalyst for Highly Efficient Rechargeable Zinc-Air Batteries[J]. Advanced Materials, 2018, 30(46):1803372-1803381.